

## The Time Mean Velocity and Temperature Fields in Developed Region in an Asymmetrically Heated Smooth Square Duct

A.K.M. Abdul Hamid\*, A. R. Akanda\*\* and M.A. Taher Ali\*\*\*

Received 24 July 2011; Accepted after revision 30 December 2011

### ABSTRACT

*The present research deals with the experimental results concerning mean velocity and temperature fields for fully developed turbulent flow through an asymmetrically heated smooth square duct with constant heat flux boundary from the bottom wall. The experiment was carried out in the Reynolds number range  $5 \times 10^4 < Re < 1 \times 10^5$ . It is seen that the mean velocity profiles near the wall bulge towards the corner along the corner bisectors and depress near the side wall along the wall bisectors producing saddle shape form instead of normal parabolic form. This indicates the presence of secondary flow and its effects gradually increases from centre towards the side wall of duct as the saddle shape behavior of the profiles becomes more and more prominent with the decrease in wall distance. This nature of velocity profiles greatly influences the temperature distribution in the flow field producing lower values of  $\Theta/\Theta_c$  near the wall. However the influence of Reynolds number on temperature is 25 percent of that on velocity. In spite of this differential influence the correlation between the velocity ratio,  $u/u_c$  and the temperature ratio,  $\Theta/\Theta_c$  curves fall on a*

---

\* Department of Mechanical Engineering, RUET, Rajshahi-6204, Bangladesh.  
E-mail: mahamid\_ruet@yahoo.com

\*\* Department of Mechanical and Chemical Engg, Islamic University of Technology,  
Board Bazar, Gazipur-1704, Bangladesh. Email: akhanda@iut-dhaka.edu

\*\*\* (Retired Prof. of Department of Mechanical Engineering, BUET, Dhaka -1000),  
Road NO.3, House NO.21/A, Flat NO. 8, Dhanmondi (RA), Dhaka-1205, Bangladesh.  
E-mail: matali@me.buet.ac.bd

*straight line indicating their similarities. But due to presence of secondary velocity the correlation remains valid up to  $u/u_c < 0.85$  in the region  $y/B < 0.52$ . Near the wall i.e.,  $y/B > 0.52$  secondary velocity changes the correlation constants. All the temperature profiles for different Reynolds number merge together near the heated wall confirming the steady state heat flow from the wall to the flowing fluid. The semi logarithmic plots of universal velocity,  $u_s^+$  vs.  $Z^+$  and temperature  $T_s^+$  vs.  $Z^+$  for each locations of  $y/B$  show that they lie on a straight line indicating the presence universal velocity distribution in the log-law-region, region  $30 < Z^+ < 250$ .*

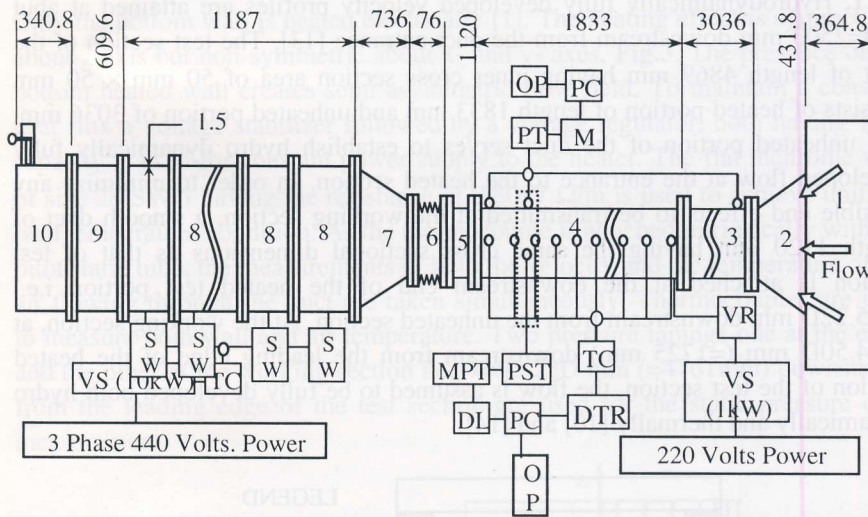
**Keywords:** Mean velocity, developed, asymmetrically, saddle shape, and secondary flow.

## 1 INTRODUCTION

Many investigators show that the flow in noncircular ducts is accompanied with secondary flow. This secondary flow not only reduces volumetric flow rate but also distorts the axial velocity field which in turn distorts the temperature field, [3], [5]. The secondary flow produces an increase in the wall shear stress towards the corners and significant influence on heat transfer at the walls. Until recently, experimental investigations of these cases were confined to comparatively simple cases with symmetrical boundary conditions. Studies of similar detail are very few in more complicated geometries with dissimilar boundary conditions. A brief literature survey indicates the lack of reliable experimental data on both velocity and temperature profiles in a square duct heated asymmetrically with constant heat flux boundary condition. An experimental study on forced convective heat transfer for smooth duct has been carried out for ten Reynolds numbers varying from  $5 \times 10^4$  to  $1 \times 10^5$  in the developed region. The object is to provide a good understanding and to obtain correlations, including Prandtl number as a variable parameter that can be used for improved numerical analysis and for better design of equipments for engineering applications [2].

Several researchers measured the primary flow velocity and got some useful results for a fully developed flow in a pipe [4], [6], [8], [14]. There are a few experimental data available for a fully developed flow through noncircular ducts [8]. The turbulent flow as well as the temperature field in non-circular ducts is influenced by the existence of the secondary flow, [5], [7]. Though the magnitude of this secondary flow is a small percentage of the primary flow

velocity, of the order of 2 to 3 percent, its influence on the flow and temperature fields in the duct cannot be ignored, [3], [6], [13]. This is why these flows and corresponding temperature fields have attracted interest not only for the light



Air Filter	8. Fans	9. Silencer	DL = Data Logger
Inlet Contractor	10. Butter Fly		PC = Personal Comput
Unheated Duct	TC = Thermo-couple		OP = Out-put
Heated Test Duct	DTR = Digital Temperature Recorder		PT = Pitot Tube
Unheated Duct	PST = Pilot Static Tube		SW = Switch
Bellow	MPT = Micro Pressure Transducer		VS = Voltage Stabilizer
Diffuser	M = Manometer		VR = Voltage Regulator

**Figure 1:** Schematic Diagram of the Setup

they shed on fluid dynamics, but also in relation to the augmentation of heat transfer, [3] [9]. The existing correlations on heat transfer for turbulent flow of air through ducts are obtained assuming Prandtl's number as a constant parameter. The present experimental study shows that the Prandtl's number drops with the increase of both the temperature of flowing air through the duct and the Reynolds number. It also drops with location of positions from the centre towards the side walls of the duct [2].

## 2 EXPERIMENTAL SET UP AND TEST PROCEDURES

The experimental set up has been made and sensing probes are installed in it and these are connected with a high speed digital computer measuring instruments. A schematic diagram of the experimental setup is illustrated in the **Fig.1**. Hydrodynamically fully developed velocity profiles are attained at about  $50D=2500$  mm downstream from the duct entrance [13]. The test section of the duct of length 4869 mm having inner cross section area of  $50 \text{ mm} \times 50 \text{ mm}$  consists of heated portion of length 1833 mm and unheated portion of 3036 mm. The unheated portion of the duct serves to establish hydro dynamically fully developed flow at the entrance to the heated section. In order to minimize any possible end effects to be transmitted at the working section, a smooth duct of length 1120 mm having the same cross sectional dimensions as that of test section is attached at the downstream end of the heated test portion i.e.,  $x=95.22D$  mm downstream from the unheated section. At the working section, at  $x=34.50D$  mm ( $=1725$  mm) downstream from the leading edge of the heated portion of the test section, the flow is assumed to be fully developed both hydro dynamically and thermally [10] and [14].

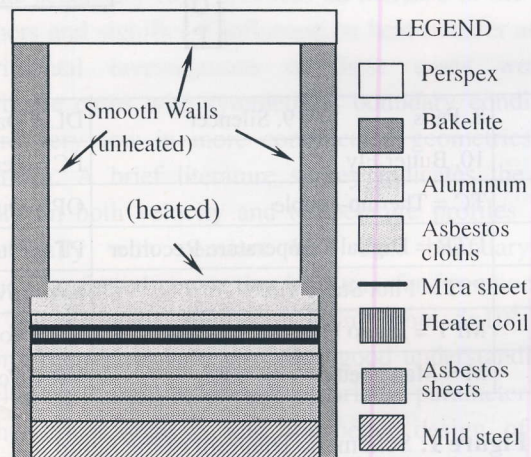


**Figure 2:** Illustrating the Cross sectional View of Duct.

**Fig.2** illustrates the details of the cross sectional view of the heated test section. Two side walls of the entire test duct are made from bakelite sheet of 12 mm thick to provide both the high strength and to ensure no leakage of current. The top wall is made from transparent Plexiglas plate of thickness 12 mm in order to provide optical access for observation and necessary adjustment of

probes. The movement of the probe is controlled by an electrical circuit which provides signals when it just touches bottom heated wall. The entire test duct except the top wall is enclosed in glass wool to minimize heat loss. The filtered air at room temperature is drawn into the straight square test duct through the air filter followed by inlet parabolic nozzle in order to establish uniform velocity. Only the bottom wall is heated electrically [1]. The heating effect is symmetrical about z-axis but non-symmetrical about x- and y- axes, **Fig.3**. The presence of the bottom heated wall creates semi asymmetric flow field. To maintain a constant heat flux a voltage stabilizer followed by a voltage regulator, both having 1kW capacity is used for constant power supply to the heater. The flat nichrome wire of size 28 SWG having the resistance of  $9.8097 \Omega/m$  is used to achieve uniform wall temperature condition. As the thermocouple is attached intrinsically with the pitot static tube, the measurements of both the velocity and the temperature of the air flowing through the duct are taken simultaneously. Thermocouples are used to measure both wall and air temperature. Two pressure tapings one at the entry and the other at the working section i.e.,  $x=95.22D$  mm ( $=4761$ mm) downstream from the leading edge of the test section are used for the static pressure drop measurement.

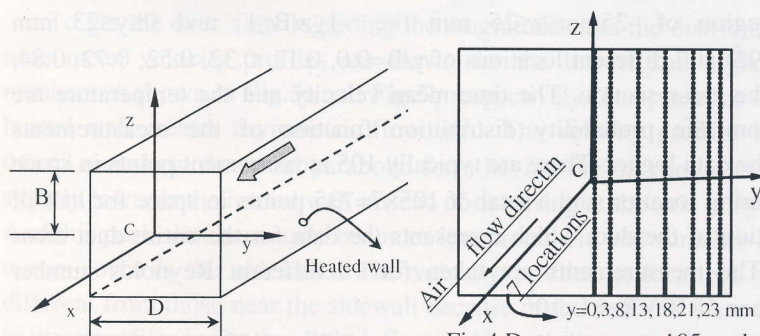


Fig: 3 Geometric Parameters and Wall Coordinate System

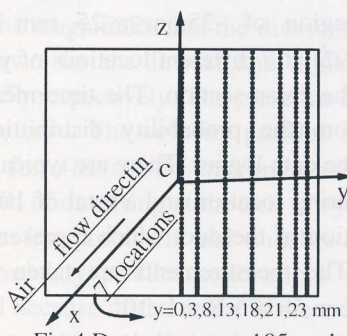


Fig:4 Dots represents 105 probe positions in space at each location

### 3 MEASUREMENT SYSTEM

The coordinate system, and the flow direction are schematically shown in **Fig.3**. The time mean velocity and the static pressure are measured by the United Sensor (USA) pitot static tube of 1.6 mm outer diameter with a Furnace Controls Ltd. (U.K), pressure transducer (model MDC FC001 and FC012 and a Keithly (USA) digital micro-voltmeter with a data logger system (model 2426). The signals of the pitot static tube are transmitted to pressure transducer through 1.4 mm bore flexible tygon tubing. The signals of the digital micro-voltmeter

correspond to the velocity head of the pitot static tube. Before starting the experiment, the output voltage for the pressure transducer for different range of scale is calibrated in the calibration rig with a Dwyer (USA) slack vertical water tube manometer for the velocity and with an Ellison (USA) inclined manometer, using Kerosene of specific gravity 0.7934, for static pressure measurement. For the measurement of all signals with micro-voltmeter, integration times of about 30 seconds are used. The bottom wall temperatures are measured by 24 copper constant thermocouples distributed along the entire length of the heated portion. The air temperature entering and leaving the heated portion are also measured by two thermocouples.

Since the duct is heated asymmetrically at the bottom wall only, it is symmetric about z-axis but asymmetric about the y-axis **Fig.3**. The measurements are taken only in one half of the cross section about the symmetrical axis as shown in **Fig.4**, which represent the flow characteristics of the entire duct. Measurements are made at the section  $x=34.5D$  downstream from the leading edge of the heated section i.e.  $x=94.56D$  from the unheated section. In this position both velocity and temperature fields can be considered to be fully developed, [10]. The time mean velocity and temperatures of air are measured within the region of  $-25\text{mm} \leq z \leq 25\text{ mm}$  (i.e.  $-1 \leq z/B \leq 1$ ) and  $0 \leq y \leq 23\text{ mm}$  (i.e.  $0 \leq y/B \leq 0.92$ ) at 7 different locations of  $y/B=0.0, 0.12, 0.32, 0.52, 0.72, 0.84,$  and  $0.92$  in the cross section. The time mean velocity and the temperature are calculated from the probability distribution function of the measurements recorded by the data logger. There are typically 105 measurement points in space at each measuring location and a total of  $105 \times 7 = 735$  points in space for half of the cross section of the duct which represents the data for the entire duct cross section [2]. The measurements are taken for 10 different Reynolds number varying between  $5 \times 10^4 < Re < 1 \times 10^5$ .

The corresponding statistical error is between 0.55 to 1.85 percent in the time mean velocity and between 1.23 to 2.06 percent in the temperature. The scattering of the wall temperature measurement is found to be between 2.0 to 3.5 percent and the uniformity of the wall temperature distribution is considered to be satisfactory, [13]. The time mean velocity measurements are repeated whenever error or doubtful situations occurred to ensure that the measured results are repeatable.

#### 4 RESULTS AND DISCUSSION

The local time mean velocity and temperature fields obtained for a turbulent flow through an asymmetrically heated smooth square duct with constant heat flux as the boundary condition are discussed briefly below:

Symbols Fig: 5a and 5b

- $y=0$ , ○  $y=3$ , △  $y=8$ ,
- ▽  $y=13$ , ◇  $y=18$ , +  $y=21$ ,
- ×  $y=23$ .

Symbols for Fig: 5c

- Re=55874, ○ Re=60666, △ Re=64029,
- ▽ Re=67490, ◇ Re=70500, + Re=74043,
- × Re=79923, \* Re=82712, - Re=85366,
- † Re=87970

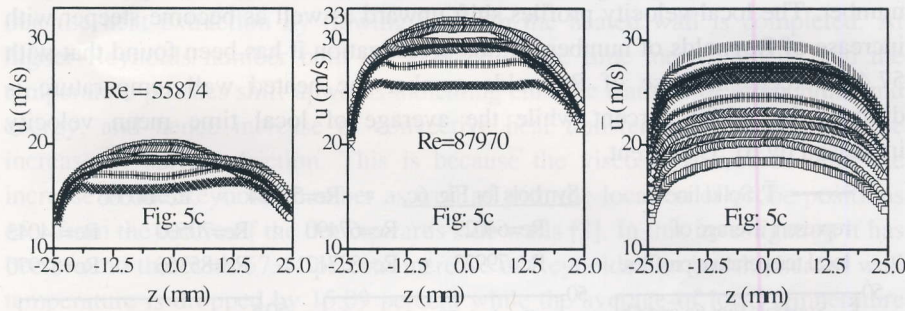


Fig: 5a and Fig: 5b Distributions of local Time Mean velocity profiles for lowest and highest Reynolds Number.

Fig: 5c Average values of local time mean velocity profiles.

#### 4.1 Local time mean velocity profiles

To get the over view regarding the magnitudes and the distributions of local time mean velocity profiles are drawn for the lowest and highest Reynolds numbers as shown in **Fig.5a** and **Fig.5b** respectively. The presence of the bottom heated wall creates asymmetric flow field. The velocity profiles in the region  $0 \leq y < 8 \text{ mm}$  show the usual parabolic form having the maximum near the centre slightly towards the heated wall instead of occurring at the axis of symmetry  $z=0$ . And this peak simultaneously becomes less prominent and vanishes as the profile moves towards the sidewalls. The velocity profiles at locations  $y < 8 \text{ mm}$  are different from those near the sidewall because of the fact that there is no bulging in these profiles indicating little influence of secondary velocity on local primary velocity in the central region of the duct. Near the sidewall  $y > 8 \text{ mm}$  the profiles show their saddle shape form in the region from  $z=-23 \text{ mm}$  near the heated bottom wall to  $z=17 \text{ mm}$  near the top unheated wall. The secondary flow carries the high velocity flow from the center towards the corner increasing the local primary velocity thereby creating this shape of the profiles. Thus the stream wise local flow velocity profiles bulge out towards the corner along the corner bisectors and depress towards the duct centre along the wall bisectors producing saddle like shape indicating the effects of secondary flow. These effects gradually increase near the side walls. Thus, towards side walls the secondary velocity on the local primary velocity profiles becomes more and more prominent and the saddle shape form of profiles from its usual parabolic form

characterizes the influence of secondary flow. The gradients of local velocity profiles near the heated wall become steeper near the side wall. It is clearly seen that the local velocity gradient is steeper near the bottom heated wall than that near the top unheated wall,

**Fig.5c** shows the local time mean velocity profiles at different Reynolds number. The local velocity profiles shift upward as well as become steeper with increase of Reynolds of number. In this investigation it has been found that with 57.44 percent increase of Reynolds number the heated wall temperature is dropped by 15.09 percent while the average of local time mean velocity increased by 61.59 percent.

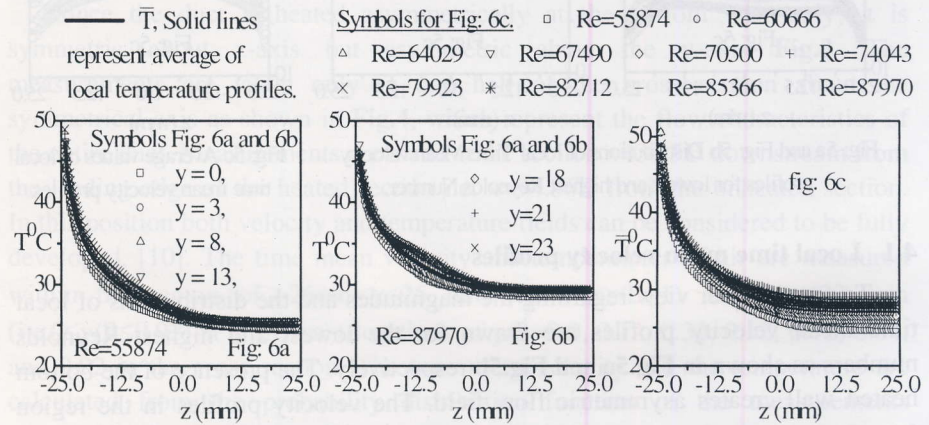


Fig: 6a and Fig: 6b Distributions of local temperature profiles for lowest and highest Reynolds Number.

Fig: 6c Distributions of average of local temperature profiles.

#### 4.2 Local Mean Temperature Profiles

**Fig.6a** and **Fig.6b** show the distributions of local temperature profiles for the lowest and highest Reynolds number. The local temperature profile remains constant in the top half cross section of the duct i.e., in the region  $25 \geq z > 0$  mm, equal to that of the entry temperature of air at the leading edge of the heated test section. This means that this region,  $25 \geq z > 0$  mm of the duct behaves like a flat plate. From approximately  $z < 5$  mm the temperature of air starts increasing at the increasing rate until the bottom heated wall where the maximum temperature is reached. The **Fig.6a** and **Fig.6b** also show that the temperature profiles in the region  $-22 < z < 0$  mm near the heated bottom wall are distorted because of the strong influence of the secondary flow enhancing turbulence intensity and hence the more heat transfer taking place in this region. This effect is greater at higher Reynolds number.

**Fig.6c** shows the comparison of the average of the local temperature profiles for ten different Reynolds number. During the experiment the room temperature varies from 24.33<sup>0</sup>C to 29.47<sup>0</sup>C because of the uncontrolled room temperature. Despite a wide variation in the inlet air temperature, all the temperature profiles near the heated bottom wall merge together which confirms that the heat extraction by flowing air from the heated wall is completed. At higher Reynolds number both the average of the time mean velocity and the temperature profiles shift upwards indicating enhance transfer of momentum and energy, and hence increase of convective heat transfer coefficients with the increase of surface friction. This is because the viscosity increases with the increase of the Reynolds number as well as with the location of probe positions of  $y$  from the centre of the duct towards side walls [2]. In this investigation it has been found that with 57.44 percent increase of Reynolds number the heated wall temperature is dropped by 15.09 percent while the average of local temperature is increased by 16.72%.

#### 4.3 Normalized Local Time Mean Velocity Profiles

At the measuring section  $x = 34.50D$ , the local time mean velocities,  $u$  at different probe positions are normalized by the central velocity  $u_c$  at  $z=0$  as  $u/u_c$ . Similarly the wall distance,  $z$  is normalized by the half width of the duct's dimension  $B = D/2$  as  $z/B$ , [10]. The plots of  $u/u_c$  vs.  $z/B$  for different  $y/B$  locations generate the normalized local time mean velocity profiles.

The normalized local time mean velocity profiles in wall coordinate are shown in **Figs.7a** to **7j**, for the smooth duct for ten different Reynolds Numbers varying in the range of  $5 \times 10^4$  to  $1 \times 10^5$ . As the flow is asymmetric the measurements are taken from the heated wall to the opposite unheated wall at seven sidewall distances of  $y/B$ . The corresponding profiles of all these figures exhibit the similar characteristics with different magnitudes of variations. The normalized local time mean velocity profiles in the region at  $y/B \leq 0.32$  show the usual parabolic form having the maximum near the centre. These profiles are showing little or no influence of secondary flow on axial velocity. The velocity gradients near the bottom heated wall are higher than those near the top unheated wall. This is because of the reasons discussed above in § 4.1. But as the position of  $y/B$  moves towards sidewall the secondary velocity on the velocity profiles becomes more and more prominent and the saddle shape form of profiles from its usual parabolic form characterizes its influence.

**Figs.9a** shows the water fall plot of the average of the time mean velocity profiles at each Reynolds Number for a clear view. Their characteristics are similar to that explained above in **Fig.5c**, § 4.1.

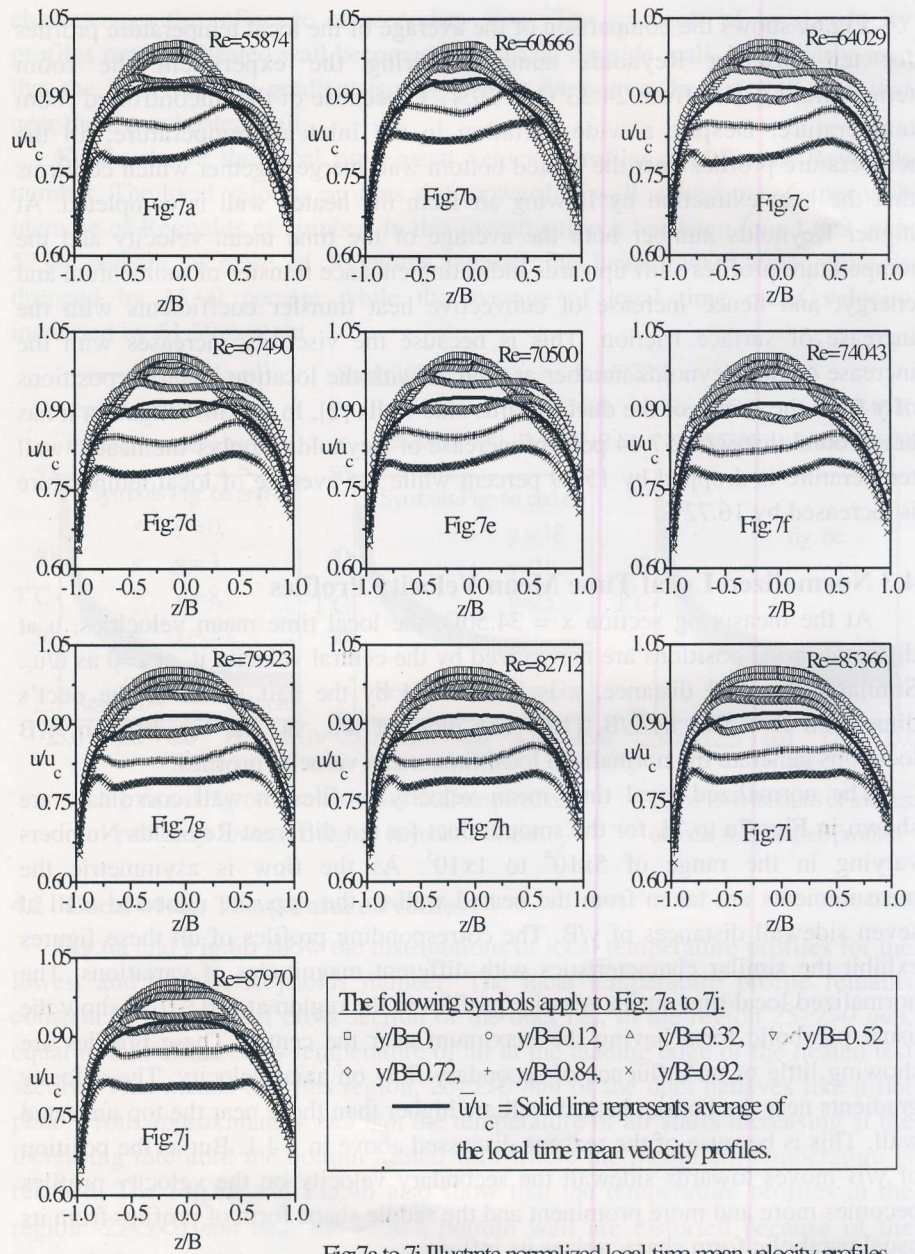


Fig. 7a to 7j illustrate normalized local time mean velocity profiles.

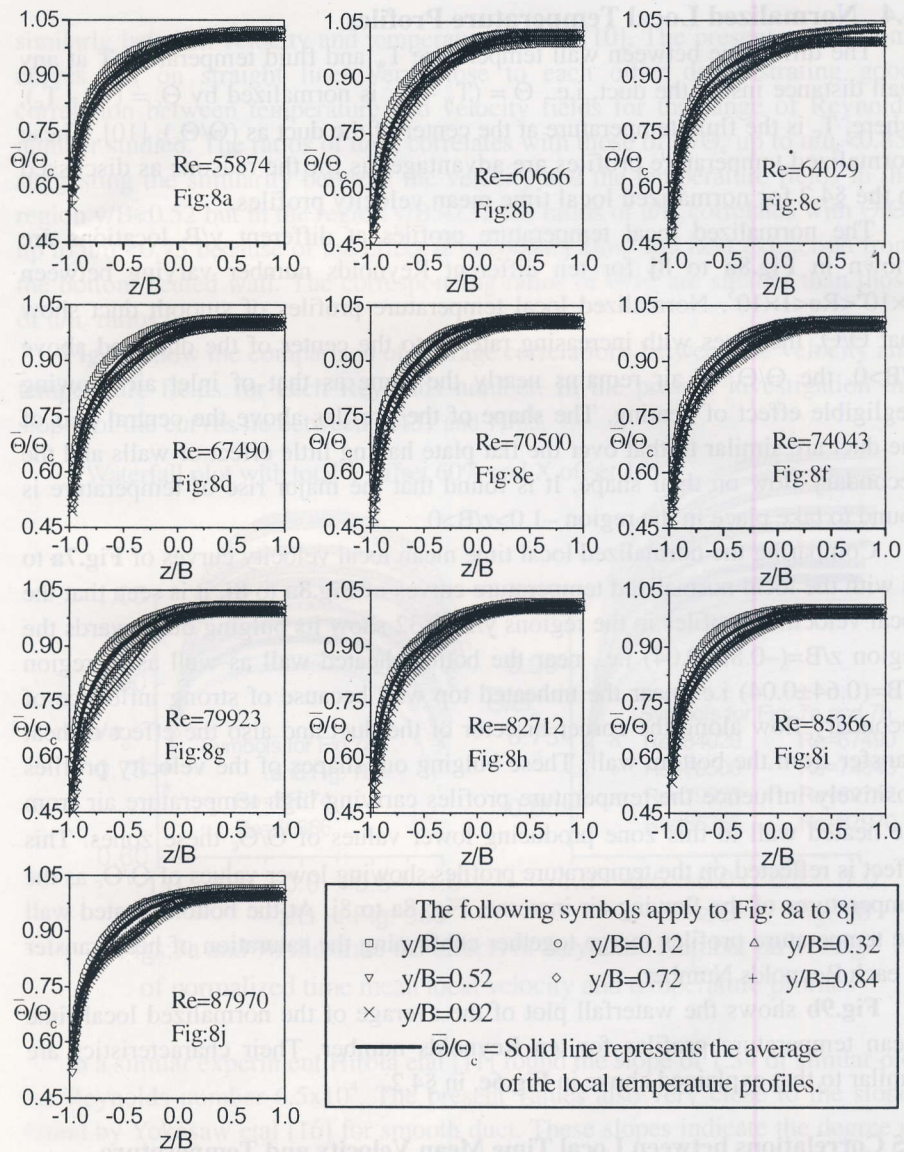


Fig: 8a to 8j Distributions of normalized temperature profiles at constant Reynolds number.

#### 4.4 Normalized Local Temperature Profiles

The difference between wall temperature  $T_w$  and fluid temperature  $T$  at any wall distance inside the duct, i.e.,  $\Theta = (T_w - T)$ , is normalized by  $\Theta_c = (T_w - T_c)$ , where,  $T_c$  is the fluid temperature at the center of the duct as  $(\Theta/\Theta_c)$ , [10]. These normalized temperature profiles are advantageous for the reasons as discussed in the §4.2 for normalized local time mean velocity profiles.

The normalized local temperature profiles at different  $y/B$  locations are shown in **Fig.8a** to **8j** for ten different Reynolds number varying between  $5 \times 10^4 < Re < 1 \times 10^5$ . Normalized local temperature profiles of smooth duct show that  $\Theta/\Theta_c$  increases with increasing rate up to the center of the duct and above  $z/B > 0$ , the  $\Theta/\Theta_c$  of air remains nearly the same as that of inlet air showing negligible effect of heating. The shape of the profiles above the central part of the duct are similar to that over the flat plate having little effect of walls and the secondary flow on their shape. It is found that the major rise of temperature is found to take place in the region  $-1.0 > z/B > 0$ .

Comparing the normalized local time mean local velocity curves of **Fig.7a** to **7j** with the local normalized temperature curves of **Fig.8a** to **8j**, it is seen that the local velocities profiles in the regions  $y/B > 0.32$  show its bulging out towards the region  $z/B = (-0.88 \pm 0.04)$  i.e., near the bottom heated wall as well as in region  $z/B = (0.64 \pm 0.04)$  i.e., near the unheated top wall because of strong influence of secondary flow along the corner bisector of the duct and also the effect of heat transfer from the bottom wall. These bulging out shapes of the velocity profiles positively influence the temperature profiles carrying high temperature air from the heated wall to this zone producing lower values of  $\Theta/\Theta_c$  these zones. This effect is reflected on the temperature profiles showing lower values of  $\Theta/\Theta_c$  as the temperatures of the flowing air increase, **Fig: 8a** to **8j**. At the bottom heated wall the temperature profiles merge together confirming the saturation of heat transfer at each Reynolds Number.

**Fig.9b** shows the waterfall plot of the average of the normalized local time mean temperature profiles for ten Reynolds number. Their characteristics are similar to that explained above in **Fig.6c**, in §4.2.

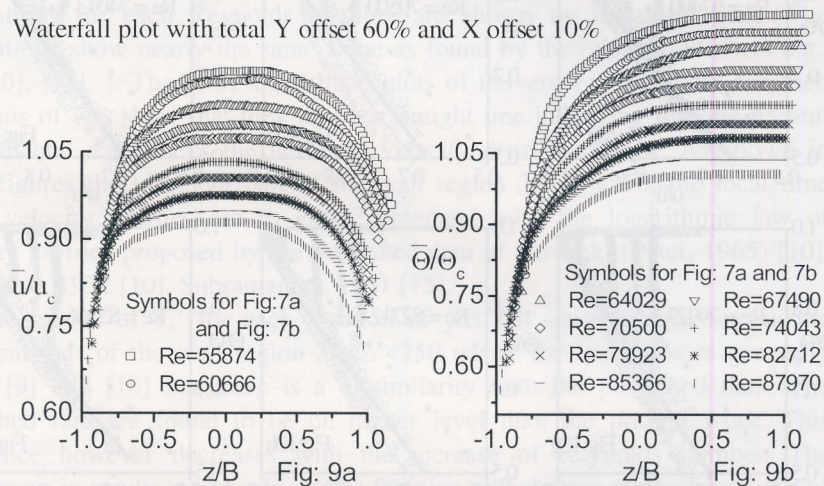
#### 4.5 Correlations between Local Time Mean Velocity and Temperature Profiles

**Fig.10a** to **10j** show the similarity between the non-dimensional velocity and the temperature fields for constant Reynolds number. If the velocity profile is in perfect agreement with that of the temperature profile then the correlation follows the straight line, [14]. Accordingly, it is plausible that the more the velocity,  $u/u_c$  correlates with the temperature,  $\Theta/\Theta_c$  the more complete is the

similarly between velocity and temperature fields, [10]. The present correlations curves fall on straight lines very close to each other demonstrating good correlation between temperature and velocity fields for the range of Reynolds number studied. The ratios of  $u/u_c$ , correlates with those of  $\Theta/\Theta_c$  up to  $u/u_c < 0.85$ , suggesting the similarity between the velocity and the temperature fields in the region  $y/B < 0.52$  but in the region  $y/B > 0.52$  the ratios of  $u/u_c$  correlates with  $\Theta/\Theta_c$  up to  $u/u_c < 0.75$  because of the effect of secondary flow and heat extraction from the bottom heated wall. The corresponding ratios of  $\Theta/\Theta_c$  are smaller than those of  $u/u_c$  ratios.

**Fig.11** show the comparison of average correlations between the velocity and temperature fields for each Reynolds number. In the present investigation the slopes of the curves lie between 1.431 and 1.135.

Waterfall plot with total Y offset 60% and X offset 10%



Figs:9a and 9b illustrate the effects of Reynolds Number on average of normalized time mean local velocity and temperature profiles

In a similar experiment Hirota et al [11] found the slope of 1.34 of similar plot for Reynolds number  $6.5 \times 10^4$ . The present values also very close to the slopes found by Yokosaw et al [16] for smooth duct. These slopes indicate the degree of similarity between the temperature and velocity fields. In the present investigation the average of the local mean correlations curves is obtained:

$$\Theta/\Theta_c = 1.287(\bar{u}/u_c) - 0.316 \quad \text{for } 5 \times 10^4 < Re < 1 \times 10^5 \text{ and } u/u_c < 0.80, \quad (\text{Fig.11}) \quad (1)$$

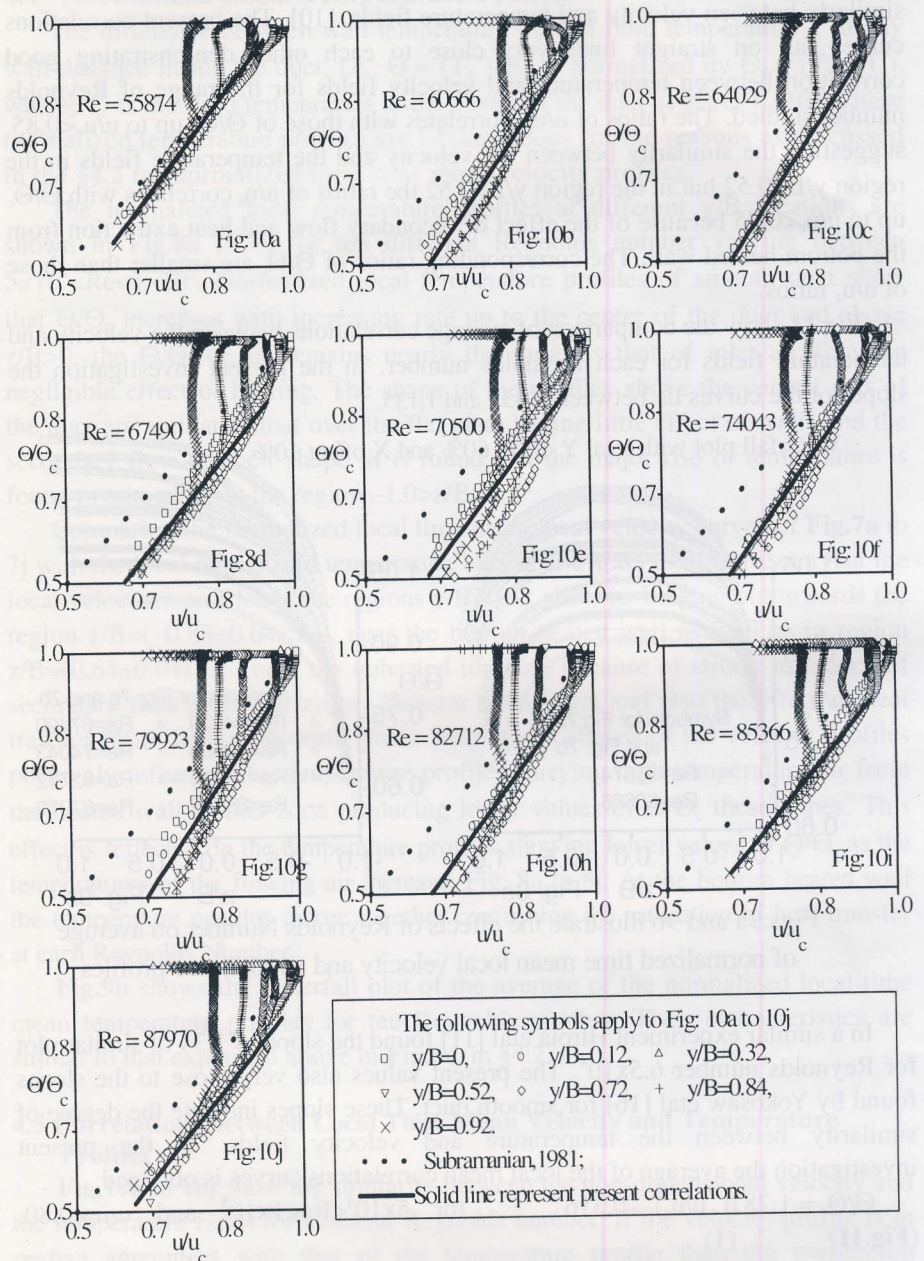


Fig. 10a to 10j Illustrate correlations between velocity and temperature profiles at Constant Reynolds number

## 5 Universal Velocity and Temperature Distributions

As both the time mean velocity and temperature of a heated flow field are of some polynomial function of the wall distance and wall temperature, their plots in simple linear scale shows in general, the characteristic of the flow field. The shape of the velocity profile in any smooth wall flow field is greatly influenced by the secondary flow, the wall shear stress  $\tau_w$  and the air density. This is because with the increase of air temperature the viscosity of air increases which intern increases the shear stress and decreases the air density [2]. Thus for the same pressure difference the velocity of the air continues to accelerate with the increase of air temperature. The universal velocity and temperature distributions are shown in **Figs.12a** to **Fig.12j** for the Reynolds number studied. In these figures, the experimental values for different  $y/B$  locations are plotted and their correlations for each Reynolds Number are shown by the solid lines. The correlations show nearly the same slope as found by the other researchers e.g., [7], [10], [11]. ). The semi logarithmic plots of universal velocity,  $u_s^+$  for each locations of  $y/B$  show that they lie on a straight line indicating that the present experimental data obeys the universal velocity distribution law. As shown in these figures the turbulent part of the wall region  $30 < Z^+ < 250$ , the local time mean velocity profiles are in good agreement with the logarithmic law of velocity profiles proposed by the published data of Sarnecki (Patel, 1965) [10], Nikuradse, 1932 [10], Subramanian, 1981 [15].

The results of  $T_s^+$  for each location of  $y/B$  fall on a straight line in the turbulent part of the wall region  $30 < Z^+ < 250$  where the inner law is generally valid, [9] and [10] but there is a dissimilarity with the published data. The published data are found to be on higher level than the present work. This difference however decreases with the increase of Reynolds number. The differences in results may be due to the fact that in their case all the four walls of their test ducts were heated while in the present experiment only the bottom wall is heated. Also the variations may be due to the different experimental setup and methodology as well as the different boundary conditions, [7] [10].

**Fig.13a** and **Fig.13b** show the comparisons of correlations for the universal velocity and temperature profiles for each Reynolds number studied. In the present investigations it is found that these correlations fall very close to each other in straight lines in the turbulent part of the wall region  $30 < Z^+ < 250$ . Hence these correlations are in good agreement with the logarithmic laws of universal velocity and temperature profiles. The semi-logarithmic laws obtained from the present experimental investigation are as follows:

$u_s^+ = 5.650 \log_{10} Z^+ + 5.211$  for  $5 \times 10^4 < Re < 1 \times 10^5$  and constant heat flux, (**Fig.13a**) (2)

$\bar{T}_s^+ = 4.638 \log_{10} Z^+ - 0.464$  for  $5 \times 10^4 < Re < 1 \times 10^5$  and constant heat flux, (Fig.13b) (3)

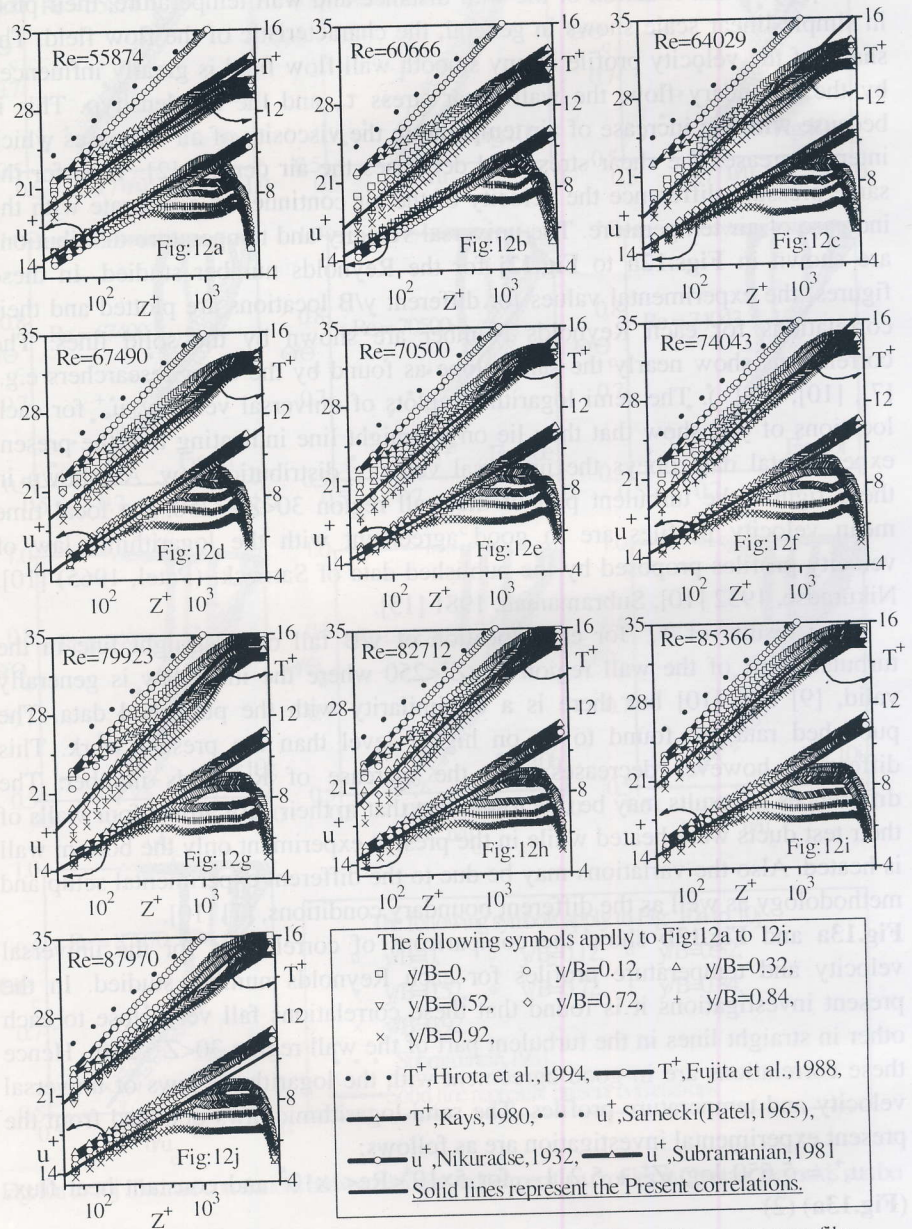


Fig: 12a to 12j: Distributions of local time mean universal velocity and temperature profiles

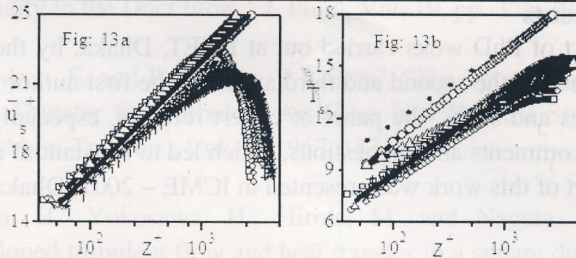
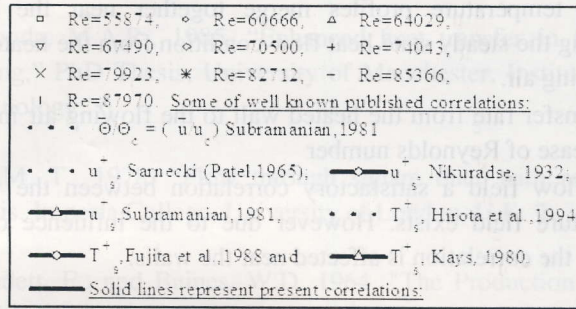


Fig. 13a and 13b Distributions of the average of the local mean universal velocity and temperature profiles.

## 6 CONCLUSIONS

In the present experimental investigation semi-symmetric (symmetric about z-axis but asymmetric about y-axis) flow field is obtained by heating bottom wall of the duct. To obtain a fully developed semi-symmetric flow field the heated part of the duct is placed at 60.72D downstream from the entrance of the symmetric duct. This ensures the developed symmetric flow condition at the entry of the heated duct. Again measurements are taken in the cross section at 34.50D downstream from the entry of the heated duct. This distance ensures the fully developed semi-symmetric flow condition in the test section. From the measurement and subsequently analyzing the results following conclusions may be made:

- (i) The flow field becomes fully developed in the measuring section.
- (ii) The mean velocity and temperature profiles obey the universal log law.
- (iii) The influence of the heated wall on the flow field is confined within the lower half ( $-1 \leq z/B \leq 0$ ) cross section of the duct.
- (iv) The influence of the secondary flow is prominent near both the walls (heated and unheated) and its effect gradually diminishes towards the centre.

- (v) All the temperature profiles merge together near the heated wall indicating the steady state heat flow condition from the heated surface to the flowing air.
- (vi) Heat transfer rate from the heated wall to the flowing air increases with the increase of Reynolds number
- (vii) In the flow field a satisfactory correlation between the velocity and temperature field exists. However due to the influence of secondary velocity the correlation is affected near the walls.

### Acknowledgments

This is a part of PhD works carried out at BUET, Dhaka, by the first author under the guidance of the second and third authors. The first author is grateful to BUET authorities and staffs, the panel of expert referees, especially the second author for their comments and suggestions, which led to substantial improvement of this work. Part of this work was presented in ICME – 2007, Dhaka.

### Nomenclature

A = Area	$m^2$	q = Heat flux	$W/m^2$
B = Half of width of duct	M	Re = Reynolds' number	Dimensionless
C = Specific heat, Centre	$W.s/kg^{\circ}C$	T = Mean temperature	$^{\circ}C$
D = Hydraulic diameter of duct	M	T* = Friction temperature	$^{\circ}C$
G = Mass flux	$Kg/m^2.s$	T <sup>+</sup> = Universal temperature	Dimensionless
h = Heat transfer coefficient	$W/(m^2, ^{\circ}C)$	u = Time mean velocity	m/s
k = Thermal conductivity	$W/(m, ^{\circ}C)$	u* = Friction velocity	m/s
L = Length	M	u <sup>+</sup> = Universal velocity	Dimensionless
P = Pressure	$N/m^2$	Z = Distance from bottom wall	mm
Pr = Prandtl number	Dimensionless	surface	
Q = Heat transfer	W	x,y,z = Coordinate system, Fig: 3 & 4	

### REFERENCES

- [1] Abdul Hamid, A.K.M.; 2004, "Experimental Study on Convective Heat Transfer with Turbulence Promoters", Ph.D. thesis, Bangladesh University of Engineering and Technology, Dhaka, Bangladesh. 1
- [2] Abdul Hamid, A.K.M.; Taher Ali, M.A. and Akhanda, M.A.R., 2007, "Characteristics Of Air Properties And Variable Parameters For Turbulent Flow In An Asymmetrically Heated Smooth Square Duct." 7th International Conference of Mechanical Engineers – 2007.

- [3] Akhanda, M.A.R., 1985, "Enhanced heat transfer in forced convective boiling," PhD Thesis, University of Manchester, Institute of Science and Technology. 6.
- [4] Ali, M. T., 1978, "Flow through square duct with rough ribs," Ph.D. Thesis, Imperia College, University of London, U.K. 7.
- [5] Brundett, E., and Baines, W.D, 1964, "The Production and Diffusion of Vorticity in the Duct Flow," J. Fluid, Vol. 19, pp. 375-394. 8.
- [6] Brundrett, E. and Burroughs, P.R. 1967, "The Temperature Inner-Law and Heat Transfer for Turbulent Air Flow in a Vertical Square duct," Int. J. Heat Mass Transfer., Vol. 10 1967, 1133. 9
- [7] Fujita, H., Yokosawa, H., Hirota, M. and Nagata, C., 1988, "Fully developed turbulent flow and heat transfer in a square duct with two rough ended facing walls", Chemical Engineering Communications, Vol. 74, pp. 95-110. 11.
- [8] Gessner, F.B., 1964, "Turbulence and Mean-flow Characteristics of Fully Developed flow in Rectangular Channels," Ph.D. Thesis, Dept. Mech. Engg. Purdue University. 12.
- [9] Gessner, F.B., and Emery, A.F., 1981, "A Length-Scale Model for Developing Turbulent Flow in a Rectangular Duct," ASME Journal of Fluids Engineering, 1981, Vol. 103, pp. 445-455. 13.
- [10] Hirota, M., Fujita, H., and Yokosawa, 1994, "Experimental study on convective heat transfer for turbulent flow in a square duct with a ribbed rough wall (characteristics of mean temperature field)," ASME Journal of Heat Transfer, Vol. 116, pp.332-340. 16-11.
- [11] Kays, W.M., and Crawford, M.E., 1980, "Convective Heat and Mass Transfer", McGraw-Hill, New York. 18-12.
- [12] Kiline, S.J., and McClintock, F. A., 1953, "Describing Uncertainties in Single-Sample Experiments," Mechanical Engineering, Vol. 75, pp. 3-8. 19-13

- [13] Komori, K., Iguchi, A., and Iguni, R., 1980, "Characteristics of fully developed Turbulent flow and Mass Transfer in a Square Duct." *Int. Chem, Eng.* 20. (2), 219-225. 20-14.
- [14] Melling, A., and Whitelaw, J.H., 1976, "Turbulent flow in a rectangular duct," *J.Fluid Mech.*, Vol. 78, part 2, pp. 289-315. 21-15.
- [15] Subramanian, C. S., and Antomia, R. A., 1981, "Effect of Reynolds number on a slightly Heated Turbulent Boundary Layer." *Int. J. Heat Mass Transf.*, Vol. 27No. 11, pp 2133- 2144. 22-16.
- [16] Yokosawa, H., Fujita, H., Hirota, M., and Iwata, S, 1989,"Measurement of turbulent flow in a square duct with roughened walls on two opposite sides." *Int. J. Heat Fluid Flow.* 2, 125-130. 23-17.

(Contd. from 2nd cover page)

8. SI units must be used in the manuscript. However, other units may be used in parenthesis.
  9. Tables should be referred to in consecutive Arabic numerical. Each table must have a table caption.
  10. Line drawings must be in a form suitable for reproduction e.g., laser printout, drawn in Indian ink on white paper or on tracing paper. Photographs should have a glossy finish. Each figure must have a number and a figure caption. Electronic mode is preferred.
  11. References should be set out in alphabetical order of the author's last name in a list at the end of the article. They should be given in standard form as in the following examples :
    - (a) Journal  
Bloomer G and Wright A. (1984) Scheduling of Vehicles from Factory to Depot. *Journal of Vehicles*, Vol. 12: pp. 590-598.
    - (b) Book  
Best, John., and Kahn, James V., Research in Education, Prentice-Hall, New Jersey, 1986.
    - (c) Monograph  
Syedali, M.M. "Computer Controlled Car", Thesis, M.Sc. Engineering, Department of Mechanical Engineering, BUET, 1990
    - (d) Conference Paper  
Hasan M and Ullah MS. "Tourism development in the Chittagong Hill Tracts of Bangladesh after the peace agreement of 1997", a paper submitted to the Regional Conference on physical mobility and development in the mountains", Tribhuvan University, 15-17, March, 2000 Kathmandu, Nepal, pp.12
    - (e) Unpublished paper  
Ahmadi, R and Tangs : Production Allocation with Dual Provisioning, Working Paper, Anderson Graduate School of Management, UCLA (1991)
  12. The University does not accept responsibility for loss or damage of manuscript while in mail.
  13. The responsibility for opinions in the contributions rests entirely on their authors.
  14. The author (s) must submit declaration that the paper was not published elsewhere.
  15. In case of joint papers, communication will be made with the first author.
  16. The University will reserve the copyright of the paper once it is accepted for publication in the Journal. The authors must obtain written permission from REASP, IUT for publication elsewhere.
- Procedure for acceptance of papers and publications :
1. Papers submitted for publication will be referred to the listed reviewers for assessment. However, the editorial board will make initial screening of the papers.
  2. After the assessment, the authors may be requested to modify/clarify certain points.
  3. Accepted/modified/corrected papers will be published in the next issue of the Journal.